Journal of Rehabilitation in Civil Engineering 11-4 (2023) 159-179

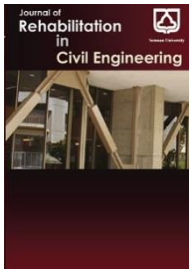

journal homepage: http://civiljournal.semnan.ac.ir/

Strength Comparison of Unreinforced Masonry Wall Made of Different Types of Brick

Mohammad Rafiqul Islam [1]; Abul Hasnat [1,*]; Raquib Ahsan [1]; Ahmed Tohameem Alam [2]

1. Department of Civil Engineering, Bangladesh University of Engineering and Technology, Dhaka 1000, Bangladesh
2. Faculty of Environment and Natural Sciences, Brandenburg University of Technology Cottbus-Senftenberg, Cottbus, 03046, Germany
* Corresponding author: *hasnat.ce@iut-dhaka.edu*

ARTICLE INFO

Article history:
Received: 12 September 2022
Revised: 27 March 2023
Accepted: 05 July 2023

Keywords:
Axial compression;
Brick masonry construction;
Clay burnt brick;
Compressive strength;
Cyclic Loading;
Load-deformation behavior;
Shear strength.

ABSTRACT

An attempt has been made in this study to correlate compressive strength, shear strength, and wall stiffness for clay burnt bricks with frog mark and machine-made bricks without frog mark. In this experimental study, 8 prisms and 8 unreinforced masonry (URM) walls (254 mm) with a size of 1524 mm X 914 mm were constructed with two different types of bricks, i.e., clay burnt brick with frog mark and machine-made brick without frog mark. Two types of mortar thicknesses 13 mm and 19 mm were used in the test specimens. The prism specimens were tested under axial compression load normal to the bed joints and the wall specimens were tested under horizontal incremental cyclic loading along with the constant axial compressive load. Lateral loading was applied using a loading control pattern. The specimens were tested under cyclic loading conditions displacing them laterally, along the axis of the walls and their load-deformation behavior was measured by dial gauges. It is observed that with increasing mortar thickness prism, ultimate strength increases 18.0% for clay burnt brick and with increasing mortar thickness prism, ultimate strength increases 1.3% for machine-made brick. On the other hand, with increasing the mortar thickness, ultimate shear strength decreases 9.6% for clay burnt brick with frog mark and with increasing mortar thickness ultimate, shear strength decreases 8.0% for machine-made bricks without frog mark. In clay burnt brick shear strength is 12.5% more than machine-made brick. With increasing the mortar thickness, ductility decreases 22.0% for clay burnt brick and 20.0% for machine-made bricks. Based on the findings, it is stated that clay burnt brick is preferable to machine manufactured brick. This study will aid in the comprehension of the behavior of both types of bricks used in masonry construction, given that masonry is a common building material.

How to cite this article:
Islam, M. R., Hasnat, A., Ahsan, R., & Alam, A. T. (2023). Strength Comparison of Unreinforced Masonry Wall Made of Different Types of Brick. Journal of Rehabilitation in Civil Engineering, 11(4), 159-179. https://doi.org/10.22075/jrce.2023.28394.1711

1. Introduction

Masonry building has been widely used around the globe since the dawn of civil engineering. For at least 10,000 years, clay bricks have been used. They were commonly used in Babylon, Egypt, Spain, South America, the United States, and other places, and were manufactured from sun-dried bricks [1]. The walls of older structures are usually made of unreinforced masonry (URM) [2]. The URM components are made up of hand-placed natural or manufactured elements, such as clay-brick, that are layered on top of each other and bonded by mortar [3]. The type of clays, molding procedures and burning affect the quality of bricks [4]. As the properties of clay vary throughout the world, it will be apparent that different kinds of bricks predominate in different regions. Most of the masonry buildings are designed primarily to resist gravity loads only since the provision for earthquake loading codes is not established [5,6]. It was observed in frequent earthquakes that older masonry structures perform poorly and most of those buildings would collapse in a major earthquake. The clay brick material is relatively heavy, brittle, of low tensile strength, and shows low ductility when subjected to seismic excitation [7,8]. Recently, Hasnat et al. (2022) conducted research to improve the strength of URM walls by retrofitting with ferrocement overlay [9]. Several common failures of URM buildings have been observed from around the world. Bruneau (1994), regrouped the failure performances as follows: lack of anchorage, anchor failure, in-plane failures, out-of-plane failure, combined in-plane, and out-of-plane effects, and diaphragm-related failures [3]. The in-plane failure is characterized by a shear crack pattern, where cracks are primarily along the mortar bed joints; some inclined cracks may also be developed [10]. This study aims to find out the shear behavior of URM walls and the variables that affect the shear capacity of URM walls such as the thickness of the masonry wall. Besides, it aimed to find out a relationship between compressive strength (which is measured by prism test) and shear strength (which is measured by shear test) of brick made of clay burnt brick with frog mark and machine-made brick without frog mark. To achieve the objectives, 8 prisms and 8 URM walls were constructed and tested. Eight prisms were constructed of two different bricks. Out of 8 prisms four prisms were made of clay burnt brick two with mortar thicknesses of 13 mm and two others with mortar thicknesses of 19 mm. Four prisms were made of machine-made bricks, two with mortar thicknesses of 13 mm and two others with mortar thicknesses of 19 mm. Eight (254 mm) URM walls with a size of 1524 mm × 914 mm were constructed for shear test and wall stiffness test. Out of 8 URM walls four walls were made of clay burnt brick and another four walls were made of machine-made bricks with two mortar thicknesses of 13 mm and 19 mm.

In prior experimental research investigations, diverse sorts of experiments were conducted on the strength assessment of clay-burnt brick and machine-made brick [11–14]. Several researches have been conducted to explore the properties of walls constructed with different types of bricks [15–19]. However, very few studies have been conducted on the comparison between these two types of bricks with the variation of mortar thickness.

The preparations of the wall consisted of two steps, at first slab was made and then the

brick wall was constructed on the slab. Prisms' compressive strength was tested by compressive loading and shear test were tested on a 127 mm wall with constant vertical loads. Walls were tested under incremental horizontal cyclic loading along with the constant vertical load. Tests were conducted under load-controlled cyclic loading. During testing, one dial gauge was used to determine the horizontal deflections of the wall. A dial gauge was installed at the top of the wall to determine the horizontal deflection of the wall. From these tests, the displacement corresponding to each cyclic load was recorded. With this recorded data load-displacement response curves were prepared to compare the results of test specimens of different walls and a relationship between prism strength and shear strength. Finally, some conclusions are drawn regarding the use of clay-burnt brick with frog marks and machine-made brick without frog marks considering the effects of mortar thicknesses.

The main objective of this study is to investigate the behavior and strength of masonry prisms with a focus on the effect of the loading direction. The findings are incorporated in evaluating the in-plane strength of masonry infills.

2. Masonry strength

2.1. Masonry compressive strength

Hegemier et al. (1978) investigated the compressive strength of concrete masonry prisms normal to the bed joint [20]. The authors found that prism strength was primarily a function of the number of bed joints and not the aspect ratio. A bond pattern was observed to influence strength. The authors recommended that prisms be constructed from four or five courses with either three or four mortar bed joints. Boult (1979) aimed to determine a relationship between the compressive strength and the height of concrete masonry prisms made of different types of masonry blocks [21]. A series of stack-bonded prisms with h/d (height-to-least lateral dimensions) of 2 to 5 were constructed for each masonry unit type. Test results showed that the compressive strength decreased as the prism height increased and the rate of decline was dependent on the block type. Boult (1979) suggested that careful consideration of the material properties of the units and grout should be considered when assembling the prisms [21]. Hamid and Drysdale (1980) studied the failure modes and strength of both the concrete and brick masonry prisms when subjected to the compression applied at designated angles concerning the bed joint [22]. It was observed that two major failures were exhibited for both un-grouted and grouted prisms: a shear mode failure along the bed or head joint and a tensile failure of the prism. The maximum prism strength was reached when prisms were compressed at an orientation perpendicular to the bed joint. According to the authors, masonry design strength must take stress orientation along the bed joint into concern.

According to Brown and Whitlock (1982), High strength grout and mortar, high tensile strength brick, and low brick coring percentage are parameters that enhance prism strength [23]. Lee et al. (1984) evaluated 82 grouted and un-grouted concrete masonry prisms in compression parallel and perpendicular to bed joints [24]. The mortar and grout strength, as well as the head mortar joint detail, had an impact on the compressive strength in the two distinct loading orientations studied. The head joint

had a considerable influence on the behavior of prisms loaded parallel to the bed joint, according to the researchers, and it was advised that the head joints be filled. The mortar strength was discovered to be an essential factor in determining the strength of prisms loaded parallel to the bed joint; using a stronger mortar resulted in a 52% improvement in prism strength. Prism strength is shown to be unaffected by considerable increases in grout strength.

Wong and Drysdale (1985) investigated prisms consisting of hollow, solid, and grouted concrete block units which were subjected to compression both normal and parallel to the bed joint [25]. Both hollow and grouted concrete block units were tested using prisms that were 2 to 5 courses high. The prisms were constructed using two kinds of blocks: a 190 mm two-cell stretcher unit and a solid 190 mm block. All prisms were built using Type S mortar and a medium-strength grout. According to the authors, the compression parallel to the bed joint is 25% less than the compression normal to the bed joint. Furthermore, they discovered that grouted and solid prisms had 35 % lesser strength than hollow prisms in both loading directions. Wong and Drysdale suggested that design guidelines should include prism characteristics in all directions of compression forces and address prisms independently [25].

Khalaf (1997) studied the strength and behavior of grouted and un-grouted prisms and blocks when compressed in both normal and parallel directions to the bed joint [26]. The finding revealed that increasing the strength of the mortar enhanced the strength of the prism in both directions of loading. However, for prisms compressed parallel to the bed joint, the impact of increasing mortar strength on prism strength was not significant. For prisms compressed normally to the bed joint, an increase in grout strength led to an increase in compressive strength, however, prisms compressed parallel to the bed joint showed a drop in strength for high-strength grout.

Haach et al. (2010) studied the compressive strength of concrete block masonry when loaded uniaxially [27]. According to their study, Due to the tensile stresses created normally to the bed joint when the specimens were loaded in compression parallel to the bed joints, cracking along the mortar-block interface was seen. The compressive strength parallel to the bed joint is around 55% of the compressive strength normal to the bed joint.

Soon (2011) investigated a concrete masonry block prism that was loaded either parallel or normally to the bed joint [28]. The prisms were grouted, partly grouted, or completely grouted with type S mortar. Hollow square prisms have better compressive strength than completely grouted square prisms when loaded parallel to the bed joint. The prisms' compressive strength was found to be roughly 50% greater when loaded normally to the bed joint than when loaded parallel to the bed joint.

2.2. Masonry shear strength

Shear strength in masonry is critical, according to Maheri (2011), since it is the primary force resisting seismic forces [29]. Because the strength of the masonry bricks is often higher than that of the mortar, failure typically happens at the connection between the bricks. Therefore, the shear bond strength is very significant [29].

Venkatarama Reddy and Vyas (2008) investigated the relationship between the shear bond strength and the compressive

bond strength [30]. The results of the shear tests indicated that there was an increase of up to four times in shear strength compared to the specimens with a smoother surface texture to the ones with a rougher surface texture, results ranged from 0.21 MPa to 0.83 MPa. Venkatarama Reddy and Vyas (2008) also noticed that failure of the interface generally occurred if the shear strength was lower than 0.25 MPa, if the shear strength was greater than 0.25 MPa then either the brick or the mortar will fail in shear [30].

Waon-Ho et al. (2004) constructed and tested seven unreinforced masonry wall specimens to study the shear behavior and capacity [31]. The investigation of test results indicates that most test walls show the primary influence of rocking mode. Because of the load concentration in the toe portion due to the rotation of the wall body, the crushing occurred at the toe portion. In the case of the slender wall, sliding due to the bed-joint crack occurs. The relationship between shear stress and vertical axial stress is proportionate in the square root pattern. The relationship between shear stress and aspect ratio shows a linear pattern. Shear stress and cross-sectional areas are not proportional.

Churilov and Dumova-Jovanoska (2010) carried out an experimental investigation of the behavior of in-plane loaded unreinforced masonry panels [32].

Ali et al. (2012) constructed and tested 108 mortar cubes, 96 masonry prisms for triplet tests, 48 masonry prisms for compression tests, and 48 masonry wallets for diagonal tension tests [33]. The effect of various mortar types (cement-sand CS, cement-khaka CK, and cement-sand-khaka CSK) and mix proportion on the mechanical properties are investigated. From the study they found, masonry bond strength, compression strength, diagonal tension strength, and elastic modulus decrease with increasing the relative proportion of sand and khaka constituent in mortar.

Voon and Ingham (2006) investigated the effects of shear reinforcement, axial compression load, type of grouting, and wall aspect ratio on masonry shear strength [34]. Axial compression load had a significant influence on the in-plane shear performance of masonry shear walls, mainly because it suppressed the tensile field in a material inherently weak in tension. Consequently, as the axial compression load increased, so did the ability of the walls to provide shear resistance.

Maheri et al. (2011) carried out several tests on half-scale brick wall panels, having different material properties, with head joints and without head joints are presented [29]. The walls were subjected to in-plane, as well as out-of-plane pushover loads to failure and their load-displacement curves were established. It was found that, depending on the material properties and the modes of failure of the wall, the head joints contribute 40% to 50% to the in-plane shear capacity of the wall.

Maheri et al. (2011) collected from field tests on brick walls of over 400 unreinforced brick buildings, situated in different parts of Iran, are comparatively analyzed to derive quantitative results regarding the main factors affecting their shear strength [29]. The results showed the important effects of the humidity level of the environment on the shear strength of brick masonry walls. A nearly two folds increase in strength can be seen for walls constructed in wetter northern parts of the country compared to the drier

central parts. It is, therefore, recommended that for assessing the vulnerability of unreinforced brick buildings, regionalization is considered and an appropriate 'region factor' is adopted.

Maheri et al. (2012) conducted experiments to determine the state of brick units' moisture content on the shear capacity of brick walls [35]. They found that the in-plane shear capacity of brick walls is more than doubled if the bricks are used in a saturated, surface dry condition, compared with naturally dried (20% moisture) condition. Based on their laboratory test results, they recommended that for strength and seismic evaluation and retrofitting studies of existing brick structures in dry regions of the world, the shear capacity of the walls constructed with dry bricks should be considered as only half of the capacity of the walls constructed with pre-wetted brick units.

3. Experimental procedure

3.1. Material properties

3.1.1. Compressive strength of machine-made bricks

The compressive strength of machine-made bricks was evaluated, and the average compressive strength of machine-made bricks was found to be 27.63 MPa.

3.1.2. Compressive strength of clay burnt bricks

The compressive strength of clay-burnt bricks was evaluated, and the average compressive strength of machine-made brick was found to be 25.27 MPa.

3.1.3. Properties of sand

Local sand has been used for masonry wall construction as well as to prepare slabs. Fig. 1 shows the gradation curve. Other properties of the sand are shown in Table 1.

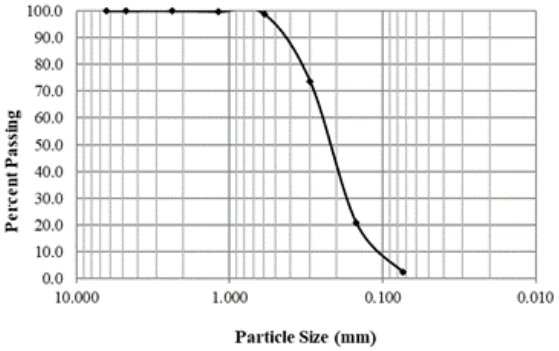

Fig. 1. Grain size analysis of sand.

3.1.4 Properties of coarse aggregate

Brick aggregate was used as coarse aggregate to prepare slabs. The gradation curve is shown on Fig. 2. Other properties of coarse aggregate are shown in Table 1.

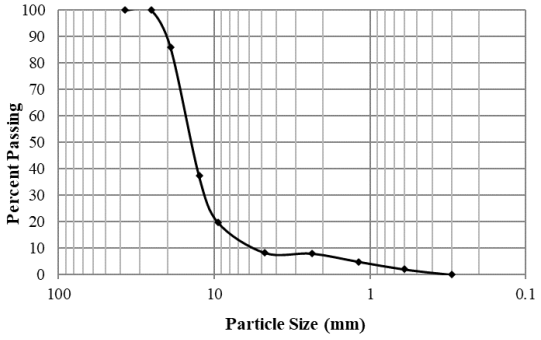

Fig. 1. Grain size analysis of coarse aggregate.

Table 1. Properties of coarse and fine aggregate.

Type of Aggregate		Specific gravity	Absorption (%)	Unit weight (SSD) kg/m^3	Absorption
Fine Aggregate	Local sand	2.24	1.23%	1295	
Coarse Aggregate	Brick Chips	1.89	13.68%	1275	33.4%

3.1.5 Cement

For the control and retrofitted specimens, CEM-I (Ordinary Portland Cement) was used. In CEM-I cement, 95 to 100% is clinker and additional constituents are 0 to 5%. Used CEM-I Conform 52.5 N Grade of BDS EN 197-1:2003 [36].

3.1.6. Properties of mortar

The average mortar compressive strength shall be determined by the cube test of mortar. A mortar mix of 1:3 (cement: sand) was used throughout this investigation. Ordinary Portland cement with finely graded sand was used for specimen preparation. The 7-, 14-, and 28-days compressive strength of mortar were found to be 13.01 MPa, 15.99 MPa, and 17.05 MPa respectively.

3.2. Test specimen preparation

Eight specimens of different bricks and mortar thicknesses were prepared for this study (Table 2). First, eight wood formworks were prepared for the construction of a masonry wall on the slab. The reinforcement 12 mm Φ bars were used as the main reinforcement of the slab. 8 mm Φ bars @ 102 mm C/C were used as perpendicular to the main reinforcement.

Table 2. Specimen details

Sample ID	Brick type	Mortar Thickness (mm)
C-1/2	Clay burnt brick with frog mark	13
C1-1/2		
C-3/4		19
C1-3/4		
M-1/2	Machine-made brick without frog mark	13
M1-1/2		
M-3/4		19
M1-3/4		

After the proper placement of reinforcement over the formwork, fresh concrete was poured over it. In the slab, 19 mm downgrade brick chips were used as coarse aggregate and Sylhet sand, 1:3 in proportion was used in the concrete mix. The mixing ratio of concrete was kept at 1:2:3 (by weight) having a water-cement ratio of 0.46 to obtain more concrete strength. Curing was done for 28 days.

3.2.1. Construction of test specimen (Masonry Wall)

There are eight masonry wall specimens that are constructed for the test. Four Masonry walls are constructed of clay burnt brick with two mortar thicknesses of 13 mm and another two-mortar thickness of 19 mm. And another four masonry walls are constructed of machine-made bricks with two mortar thicknesses of 13 mm and 19 mm.

3.2.2. Construction of test specimen (Masonry Prism)

There are eight masonry prisms that are constructed for the test. Four masonry prisms are constructed by clay burnt brick two with mortar thickness of 13 mm and two with mortar thickness of 19 mm. Another four masonry prisms are constructed by machine-made bricks, two with mortar thickness of 13 mm and another two with mortar thickness of 19 mm.

3.2.3. Construction of test specimen (Masonry Prism)

There were eight masonry prisms constructed for the test. Four masonry prisms are constructed by clay burnt brick two with mortar thickness of 13 mm and two with mortar thickness of 19 mm. Another four masonry prisms are constructed by machine-made bricks, two with mortar thickness of 13

mm and another two with mortar thickness of 19 mm.

3.2.4. Prism test setup

After 28 days of casting prism, the compressive strength of the prisms was determined by compressive loading. The test setup of masonry prisms is done.

3.2.5. Experimental shear test setup

There are four types of eight masonry walls constructed for the shear test. The shear test was done with a 127 mm wall. Shear test on two walls C-1/2 and C1-1/2, i.e., Clay burnt brick wall with mortar thickness 13 mm was performed with three (3) ton vertical loads. Another six (6) walls were performed with 6-ton vertical loads. Out of 6 walls, two were made of clay-burnt bricks with mortar thickness of 19 mm, and the other four were made of machine-made bricks with mortar thickness of 13 mm and 19 mm. A hand grinding machine, hammer and chisel were used for cutting the wall and setting up the shear test arrangement.

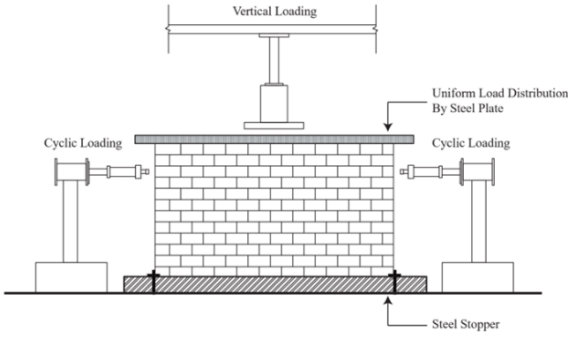

Fig. 3. Schematic diagram of loading condition during the test.

3.2.6. Experimental setup of wall stiffness, testing procedure, data acquisition

The models were placed on a steel base and laterally fixed by anchoring the wall. The base plate was fixed on a steel beam which was fixed with the concrete floor as shown in Fig. 3. There are two hydraulic jacks manually operated to provide an axial load on the top of the wall, and another two hydraulic jacks leftward and rightward direction to provide a lateral load on the wall.

The wall specimens were tested under horizontal incremental cyclic loading along with the constant axial load. Lateral loading was applied using a loading control pattern. The specimens were tested under cyclic loading conditions displacing them laterally, along the axis of the walls. Loading and unloading were applied in 0.5-ton increments in the positive (leftward) and negative (rightward) direction for every cycle. Whereas 2-ton, 3-ton, 4-ton, 5-ton, 7-ton, 9-ton and 10-ton loading increments were maintained for 1st, 2nd, 3rd, 4th, 5th, and 6th cycle. A constant loading rate per cycle was maintained until the specimens experienced a significant loss of capacity.

3.3. Load selection

The specimen walls were tested under incremental cyclic loading along with a constant axial load of 6% of prism strength. The wall specimen of clay burnt brick with a mortar thickness of 13 mm was tested with 3-ton axial loads. Two wall specimens of clay burnt brick with mortar thickness of 19 mm and another four specimen walls made of machine-made bricks were tested with 6-ton axial loads. The axial load was kept constant throughout the experiment of each specimen. The static cyclic loading had been provided by two hydraulic jacks. The load had been controlled by measuring the horizontal displacement of the wall for cycle I, cycle II, cycle III, cycle IV, cycle V, and cycle VI, respectively.

3.4. Testing procedure

Before testing all the specimens were whitewashed to find out the crack and their absolute location. Precautions were taken to avoid any potential damage during the lifting and transporting of the specimens. The specimens had been lifted by a series of pulleys and set on the base plate. One hydraulic jack was set in the position at the top of the column to apply constant axial loading. Another two hydraulic jacks were linked to the left side and right side of the specimen wall along its length to apply incremental cyclic loading. The dial gauges were set in position. At first 6-ton axial load was applied on the top of the wall and kept constant throughout the test. After applying the axial load, the initial dial gauge reading was taken as reference points to measure the deflections of the wall. Then the incremental cyclic loadings were applied by the left and right jacks simultaneously and progressive readings were taken. The loading and unloading of the hydraulic jacks were controlled manually. Fig. 4 shows the experimental setup before starting the wall stiffness test.

Fig. 4. Experimental setup before starting the test.

4. Results and Discussion

All eight samples of the wall were subjected to constant axial load throughout the shear test and incremental cyclic loading in the stiffness test of the wall. Eight prism test specimens were tested by compressive loading. Sample Due to malfunction, the M1-3/4 sample did not work perfectly. This specimen is discarded from the conclusions made in the later discussions. Dial gauges were used to measure the deflection of the wall.

4.1. Failure modes of wall specimen

4.1.1. Load – deformation response

Load-deformation responses of all seven specimens were monitored by dial gauges throughout each test specimen. Dial gauges were placed at the top of the wall to record the lateral displacement. Testing was terminated when the specimen failed. Fig. 5 to Fig. 11 provides the load-deformation responses of each specimen. From the figures, it can be observed that specimens made of clay burnt brick with mortar thickness 19 mm (Type C-3/4 and C1-3/4) gave almost the same highest loading which is done by 6-ton vertical loads, and clay burnt brick with mortar thickness 13 mm (type C-1/2 and C1-1/2) was performed by 3 tons vertical loads. This represents the more ductile quality of clay-burnt brick walls.

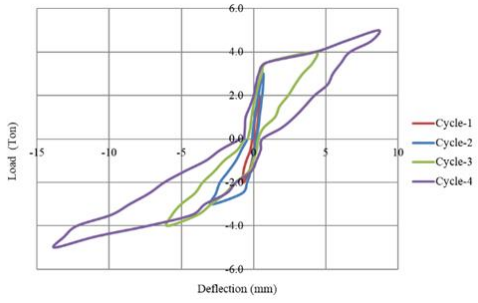

Fig. 5. Load deformation response of sample wall C-1/2.

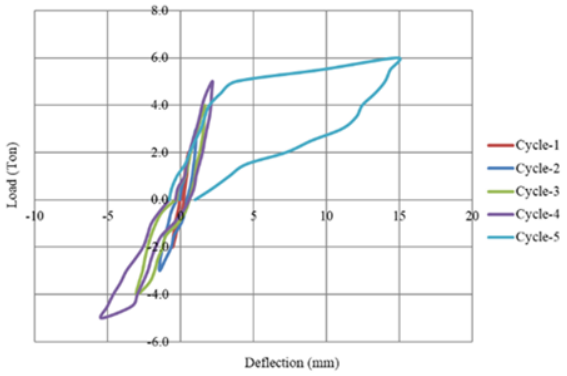

Fig. 6. Load deformation response of wall C1-1/2.

Nevertheless, type C-3/4 and C1-3/4 specimen undergo larger deformations without rupture before failure than type C-1/2 and C1-1/2 specimen. Also, type C-1/2 and C1-1/2 specimen undergo larger deformations without rupture before failure than type M-1/2 and M1-1/2 specimen. The maximum load of (the type C-3/4 and C1-3/4) samples was 9 to 10 tons, whereas for (type C-1/2 and C1-1/2) samples it was 5 to 6 tons, for (type M-1/2 and M1-1/2) sample it was 6 tons and type M-3/4 sample it was also 6 tons. The maximum displacement of type C-1/2 and C1-1/2 samples under loading were 14.38 and 15.68mm respectively. Whereas for type C-3/4 and C1-3/4 sample maximum displacements were 13.11 mm and 15.80mm. For type M-1/2 and M1-1/2 samples, maximum displacements were 15.4 mm and 13.47mm. And for the type M-3/4 sample, maximum displacement was 20.89mm. The hysteresis loop of the type M1-1/2 specimen has an abnormal result. So that only the result of machine-made brick with mortar thickness of 13 mm type M-1/2 was used and the result of type M1-1/2 specimen was rejected.

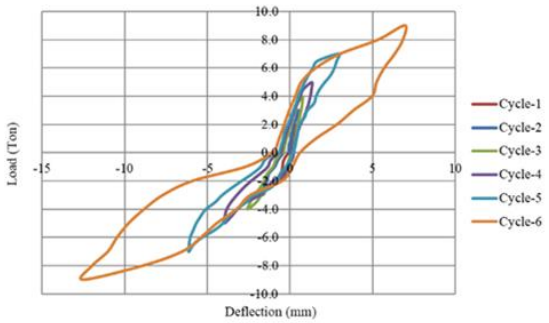

Fig. 7. Load deformation response of specimen wall C-3/4.

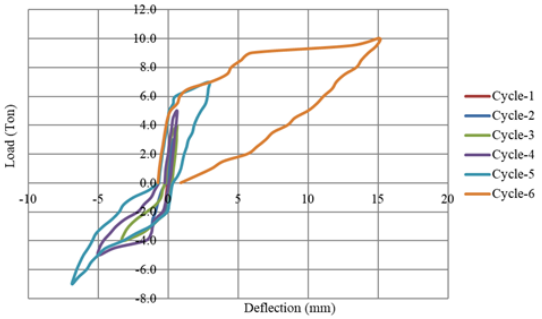

Fig. 8. Load- deformation response of specimen wall C1-3/4.

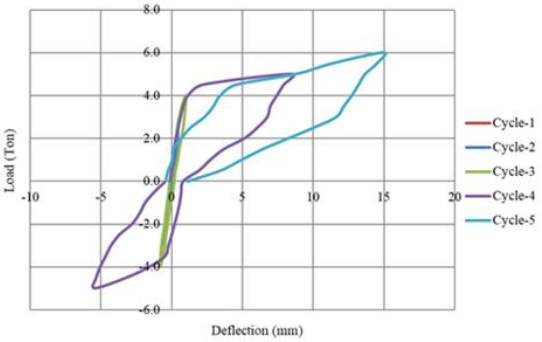

Fig. 9. Load- deformation response of specimen wall M-1/2.

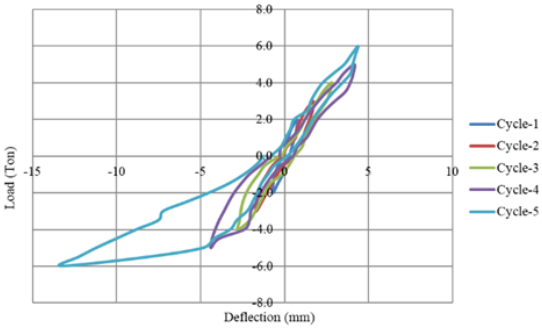

Fig. 10. Load- deformation response of specimen wall M1-1/2.

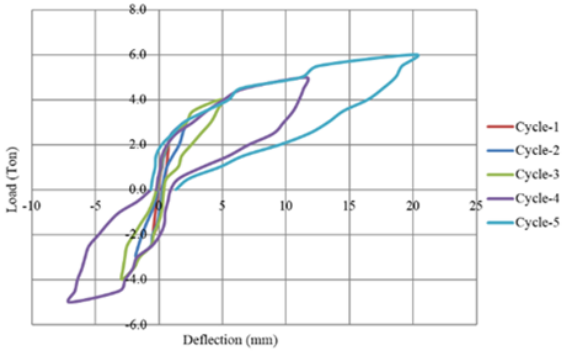

Fig. 11. Load- deformation response of specimen wall M-3/4.

The hysteresis loop envelopes of seven samples are shown on Fig. 12. In every case, with the increase of mortar thickness, displacement was reduced with loading for both clay-burnt brick and machine-made brick.

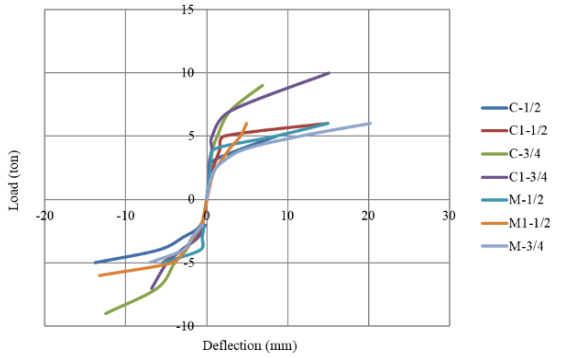

Fig. 12. Hysteresis Loop Envelopes of seven wall samples

4.2. Summary of test results of seven specimens

4.2.1. Characteristics of first crack formation

For specimens, C-1/2 and C1-1/2 first crack occurred at 2.0 tons and 2.5 tons when displacements were 0.72 mm and 1.03 mm respectively. For specimens, C-3/4 and C1-3/4 first crack occurred at 3.0 tons and 2.5 tons with displacements of 1.65mm and 0.91 mm respectively. For specimens M-1/2 and M1-1/2, the first crack occurred at 2.5 tons and 2.5 tons with displacement of 0.46 mm and 1.24 mm respectively. For specimen M-3/4 the first crack load was 2.0 tons with a displacement of 0.67 mm at 1st cycle. The load at the first crack formation of all seven samples is visualized on Fig. 13. The First crack was initiated at the wall slab connection for all the specimens.

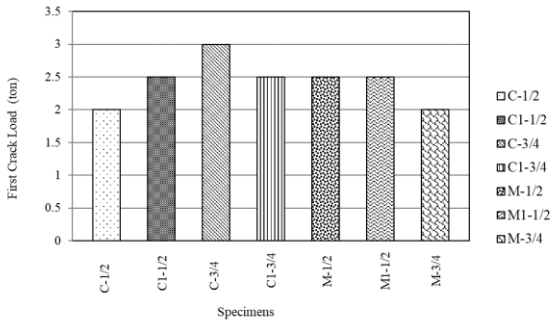

Fig. 13. Load at First Crack Formation of Seven Specimens.

4.2.2. Stiffness of specimens

The average stiffness obtained for the two half cycles in a hysteretic loop, gave the approximate stiffness for that cycle. The values of the secant stiffness obtained for each cycle are plotted for all the specimens. The degradation of the secant stiffness was plotted as the ultimate stiffness versus the corresponding cycle number for each specimen tested. Fig. 14 shows the secant stiffness of each cycle. Fig. 15 shows a degradation of stiffness of each cycle.

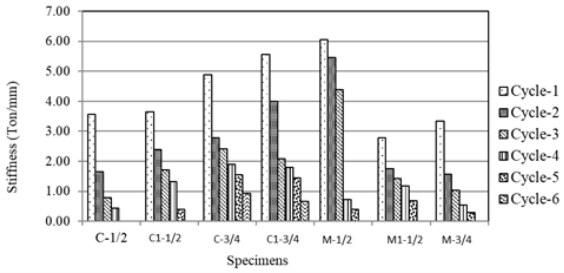

Fig. 14. Secant stiffness of each cycle for seven samples.

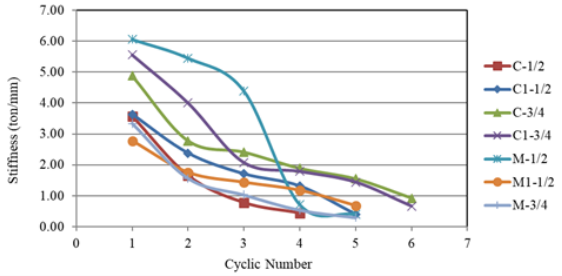

Fig. 15. Degradation of stiffness of each cycle for seven sSpecimens.

It can be noted that as the number of cycles increases, stiffness decreases. Here the stiffness of clay-burnt brick with mortar thickness of 19 mm (C-3/4 and C1-3/4) is stiffer than clay-burnt brick with mortar thickness of 13 mm (type C-1/2 and C1-1/2) because clay burnt brick wall with mortar thickness 13 mm was tested with 3-ton vertical loads and clay burnt brick with mortar thickness 19 mm was tested with 6-ton vertical loads. The value of stiffness of machine-made brick with a mortar thickness of 13 mm (type M-1/2 and M1-1/2) is stiffer than machine-made brick with a mortar thickness of 19 mm (type M-3/4). The result of the type M1-1/2 specimen was rejected because of an abnormal result. Stiffness after the first cycle and final cycle is shown in Fig. 16 and Fig. 17.

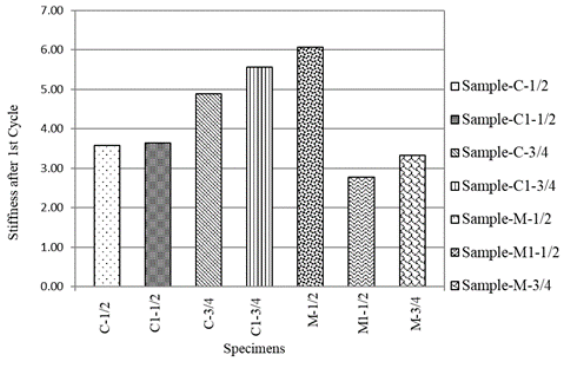

Fig. 16. Stiffness after 1st cycle of seven samples.

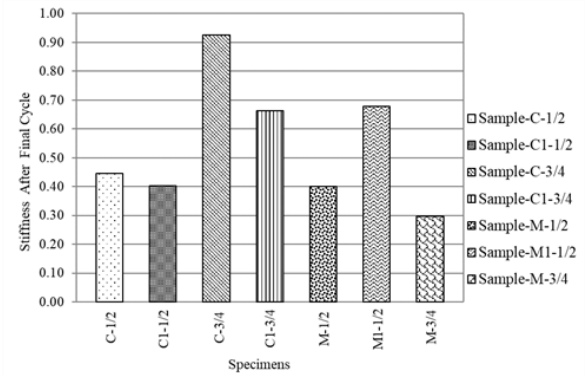

Fig. 17. Stiffness after the final cycle of seven samples.

The increase in stiffness between different categories at the first cycle and final cycle are shown in Fig. 18 and Fig. 19. For type C-1/2 and C1-1/2 stiffness varies from 3.57 to 0.45 and 3.64 to 0.40 whereas for type C-3/4 and C1-3/4 it varies from 4.88 to 0.93 and 5.56 to 0.66. Again, for type M-1/2 stiffness varies from 6.06 to 0.40 whereas for type M-3/4 it varies from 3.33 to 0.30.

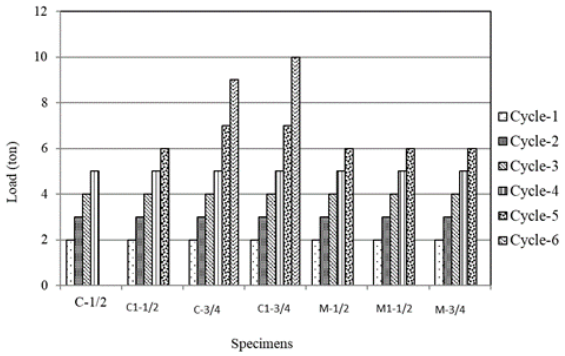

Fig. 18. The load of the specimens at every cycle.

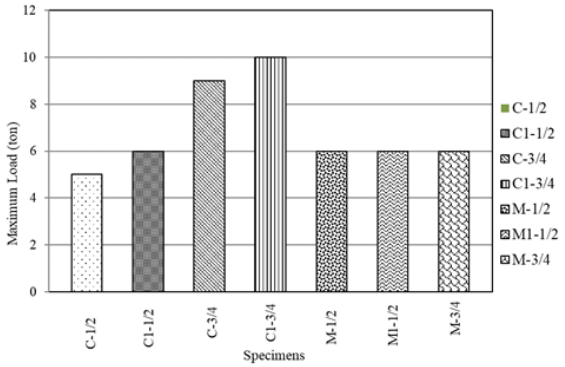

Fig. 19. Maximum load of seven specimens.

4.2.3. Maximum displacement

Fig. 20 represents the maximum displacement of every specimen of different types during loading and unloading. It was found that the maximum displacements were increased with the increasing mortar thickness. Almost all the walls (except C1-1/2, shear failure) showed flexure-type failure at ultimate load.

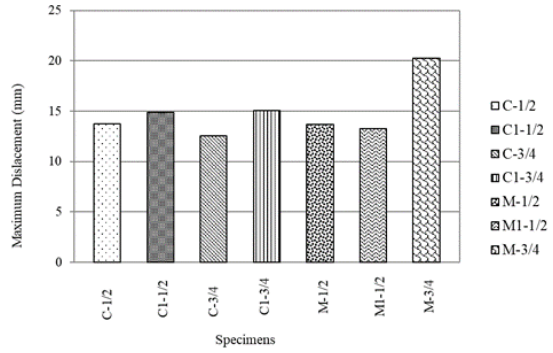

Fig. 20. Maximum displacement of seven specimens.

4.2.4. Residual displacement

It was found that the residual displacements were decreasing with the increasing mortar thickness. Fig. 21 represents the residual displacement of all seven specimens.

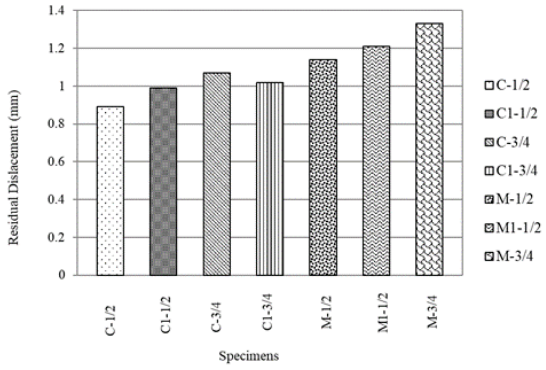

Fig. 21. Residual displacement of seven specimens.

4.2.5. Ductility of the specimen wall

Displacement ductility is obtained experimentally from the idealized bilinear approximation to the monotonic spine or cyclic peak envelope of the load-displacement curve shown in Fig. 20 to Fig. 24. Displacement ductility is defined as the ratio of deformation at a given response level to the deformation at ideal yield [37]. Here, the ductility was measured using the relationship $\mu = \Delta_{max}/\Delta_{y,}$ where Δ_{max} maximum deformation of loop and Δ_y deformation while yielding. Fig. 22 shows the ductility of all the specimens.

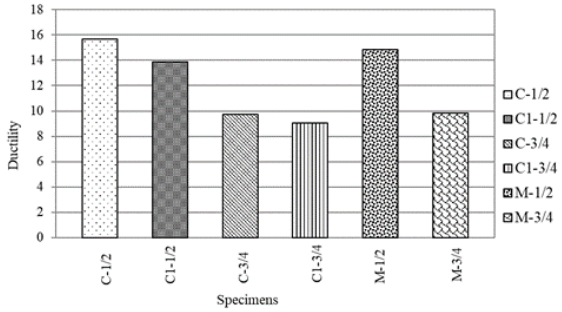

Fig. 22. Ductility of specimens.

4.2.6. Stiffness degradation calculation

Stiffness degradation has been calculated by measuring the slope of each cycle. The slope is calculated by positive and negative pick points of each loop. Sample stiffness degradation calculations are shown on Fig. 23 and Fig. 24. Fig. 25 shows the stiffness degradation of each specimen.

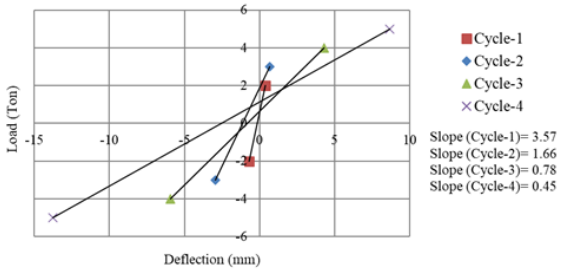

Fig. 23. Stiffness degradation of specimen C-1/2.

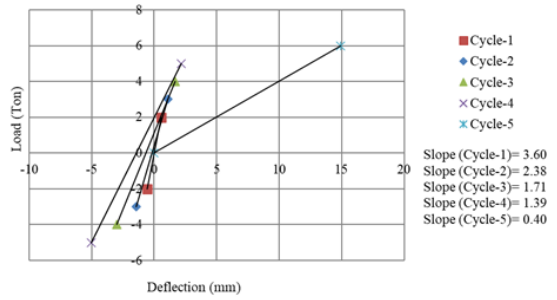

Fig. 24. Stiffness degradation of specimen C1-1/2.

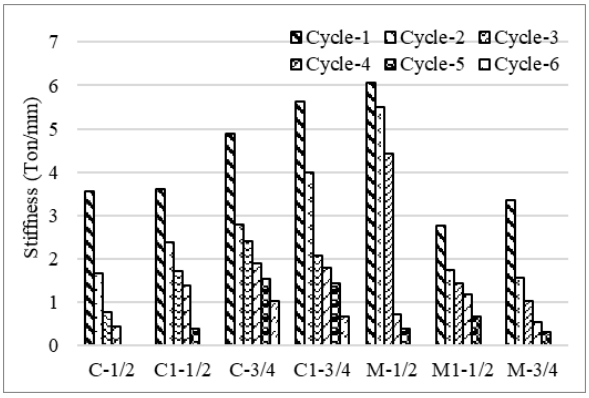

Fig. 25. Stiffness degradation of all specimens.

4.2.7. Energy dissipation calculation

Energy dissipation has been calculated by measuring energy, i.e. area of each cycle (Fig. 26 and Fig. 27). From Fig. 28, showing energy dissipation, it can be observed that energy absorbed by machine-made brick wall with mortar thickness of 13 mm is 73.6% of the total energy absorbed by machine made brick wall with mortar thickness 19 mm. It seems that with the increasing mortar thickness energy dissipation increases.

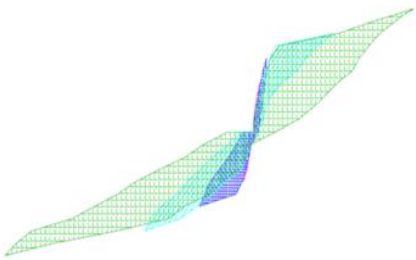

Fig. 26. Energy Dissipation calculation of specimen C-1/2.

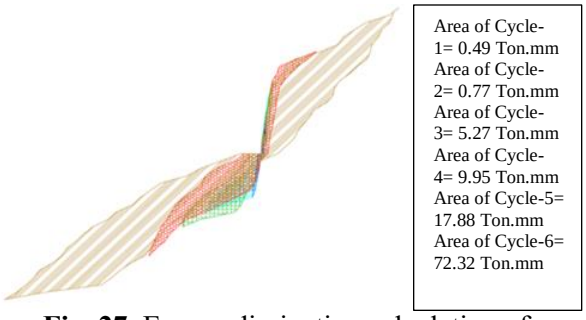

Fig. 27. Energy dissipation calculation of specimen (C-3/4).

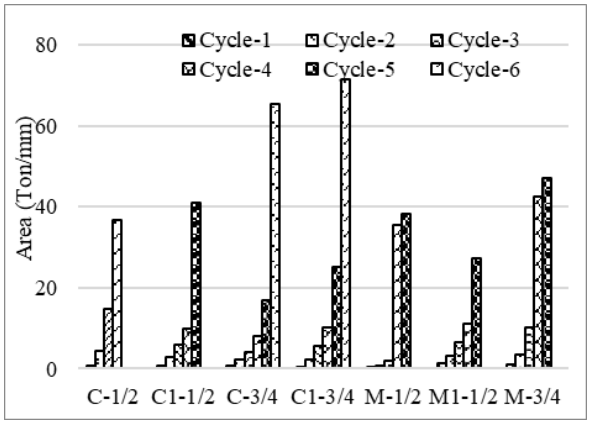

Fig. 28. Energy dissipation calculation all specimens.

4.3. Hysteresis damping

A calculation of comparable viscous damping is performed in this investigation using the theory developed by Hose and Seible (1999) [38]. Equation (1) yields the equivalent viscous damping ratio, ξ_{eq}, for the complete asymmetric cycle at a given force intensity. Fig. 29 clarifies it once further. Here the damping energy loss or energy input for the push-half cycle of the hypothetical force-displacement loop is represented by area E_{d1}. Similarly, E_{d2} depicts the energy loss during the pull half cycle. The hatched sections in Fig. 30 designate E_{s1} and E_{s2}. Strain energy is stored in an equivalent linear elastic system during the push and pull half cycles, which is represented by the above theorem.

$$\xi_{eq} = \frac{1}{4\pi}\left(\frac{E_{d1}}{E_{s1}} + \frac{E_{d2}}{E_{s2}}\right) \quad (1)$$

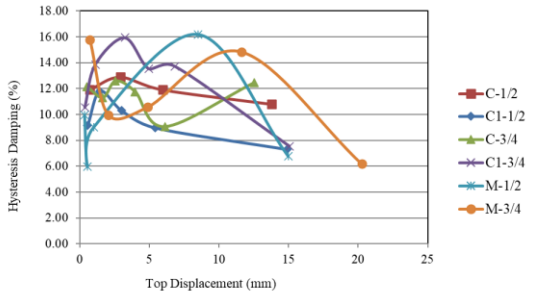

Fig. 29. Hysteresis damping percentages for wall assemblies.

The hysteresis damping was plotted against lateral top displacement for the wall shown on Fig. 29.

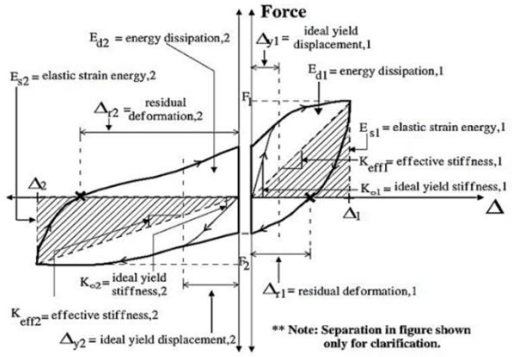

Fig. 30. Equivalent viscous damping ratio (ξeq) for asymmetric hysteresis loops [20].

4.4. Relationship between prism strength, shear strength, lateral load

Different relationships relating to different parameters are drawn from Fig. 31 to 39. To identify the relation between the latter load and prism strength; lateral load and shear strength, the result of type M1-1/2 was rejected because of an abnormal result. Machine-made brick wall with mortar thickness 13 mm only type M-1/2 result was accepted.

From the prism test of clay burnt brick and machine-made brick, prism cracking strength and ultimate strength increases with increasing mortar thickness and prism compressive strength is more than shear strength in both types of bricks. On the other hand, from the shear test of clay burnt brick and machine-made brick, cracking shear strength and ultimate shear strength decreases with increasing mortar thickness and shear strength is less than prism compressive strength in both types of bricks.

It was observed that, with the increasing mortar thickness for both clays burnt brick with frog mark and machine-made brick without frog mark, prism cracking strength and ultimate strength increases. In another hand, with the increasing mortar thickness for clay burnt brick with frog mark and machine-made brick without frog mark, shear cracking strength and ultimate strength decreases.

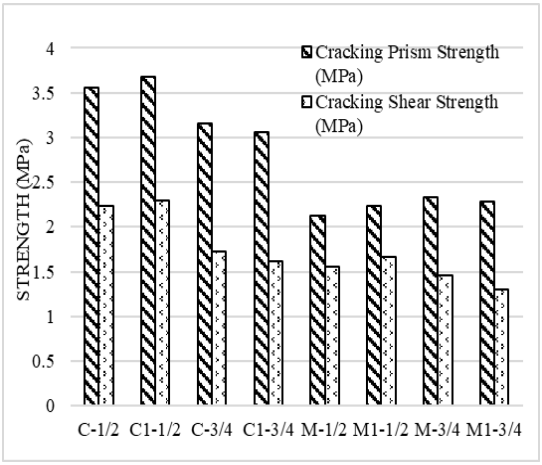

Fig. 31. Relationship between cracking prism strength and cracking shear strength.

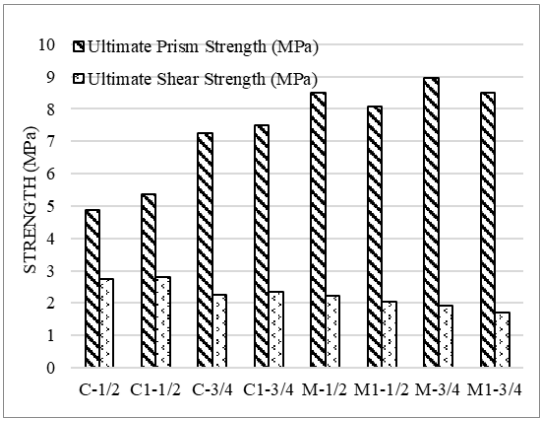

Fig. 32. Relationship between ultimate prism strength and ultimate shear strength.

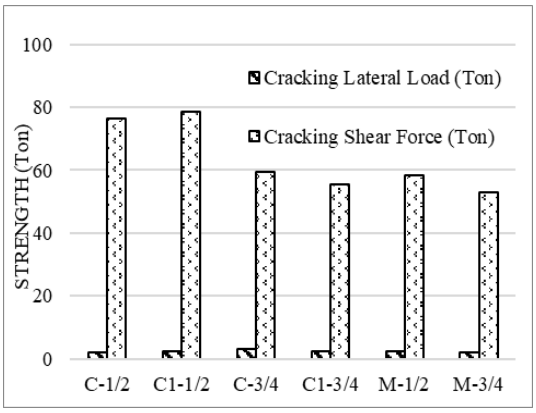

Fig. 33. Relationship between cracking lateral load and cracking shear force.

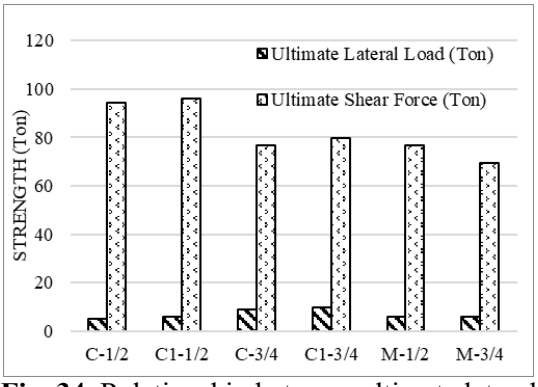

Fig. 34. Relationship between ultimate lateral load and ultimate shear force.

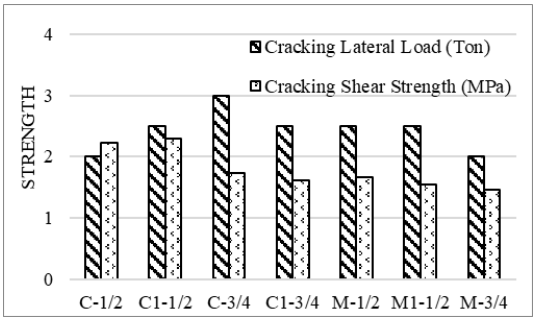

Fig. 35. Relationship between cracking lateral load and cracking shear strength.

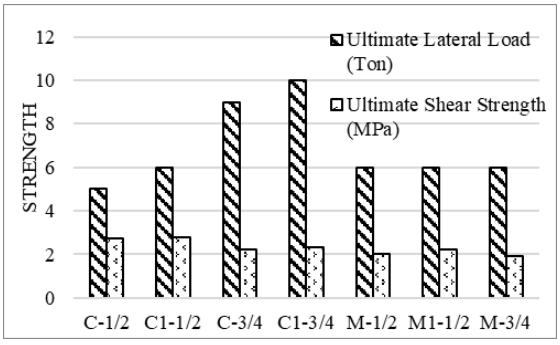

Fig. 36. Relationship between ultimate lateral load and ultimate shear strength.

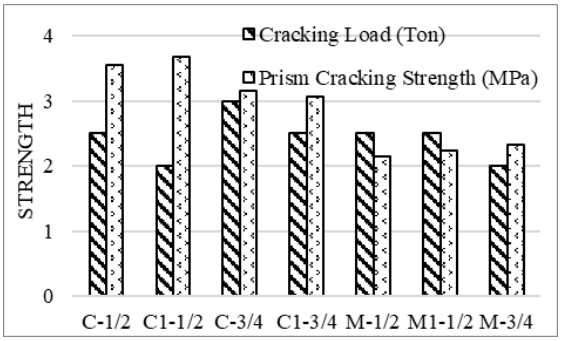

Fig. 37. Relationship between cracking load and prism cracking strength.

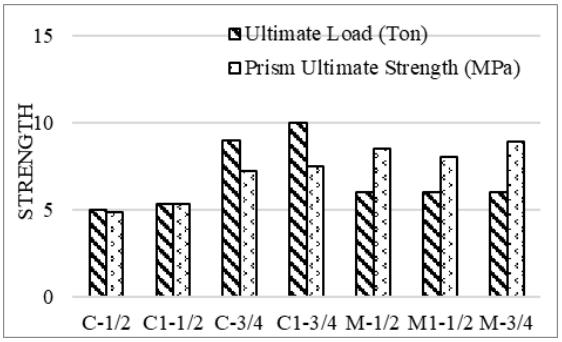

Fig. 38. Relationship between ultimate load and prism ultimate strength.

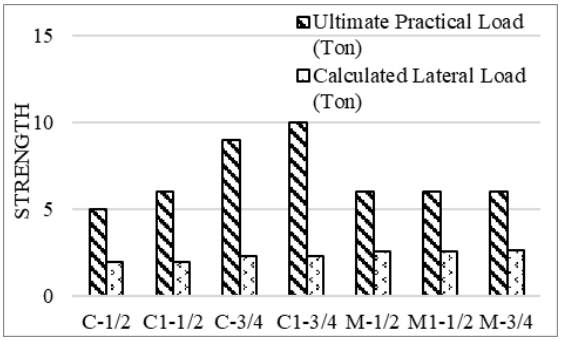

Fig. 39. Relationship between ultimate practical load and calculated lateral load.

5. Conclusions

The behavior of the walls under cyclic loading, the prism, and the shear test specimens experimented on the study were investigated. Based on the results obtained from the experiments of the specimens, the following observations can be drawn:

Increasing mortar thickness prism cracking strength and ultimate strength increases in both types of brick i.e., clay burnt brick with frog mark and machine-made brick without frog mark. Increasing mortar thickness, cracking shear strength and ultimate shear strength decreases in both types of brick i.e., clay burnt brick with frog mark and machine-made brick without frog mark. In clay burnt, brick cracking prism strength is more than machine-made brick. In, machine-made brick's ultimate prism strength is more than clay-burnt brick. In clay-burnt brick shear strength is more than machine-made brick. The specimen is made of clay burnt brick with a mortar thickness of 13 mm, the average cracking shear strength is 62.6% of average cracking prism strength and the average ultimate shear strength is 54.4% of average ultimate prism strength. The specimen is made of clay burnt brick with a mortar thickness of 19 mm, the average cracking shear strength is 53.9% of average cracking prism strength and the average ultimate shear strength is 31.0% of average ultimate prism strength. The specimen is made of machine-made brick with a mortar thickness of 13 mm, the average cracking shear strength is 72.7% of the average cracking prism strength and the average ultimate shear strength is 25.9% of the average ultimate prism strength.

The specimen is made of machine-made brick with a mortar thickness of 19 mm, the average cracking shear strength is 59.9% of average cracking prism strength and the average ultimate shear strength is 20.7% of average ultimate prism strength. Increasing mortar thickness of both types of specimen's wall ductility decreases. The average stiffness degradation of clay burnt brick with mortar thicknesses 13 mm and 19 mm are 20.0% and 13.93% per cycle respectively. The average stiffness degradation of machine-made brick with mortar thicknesses 13 mm and 19 mm is 18.68% and 18.21% per cycle. Energy absorbed by machine-made brick walls with a mortar thickness of 19 mm is 58.1% of the energy absorbed by machine-made brick walls with a mortar thickness of 13 mm. For the specimens made of clay burnt brick with mortar thickness 13 mm (Specimens- C-1/2 and C1-1/2), the average cracking lateral load is 2.90% of the average cracking shear force and the average ultimate lateral load is 5.77% of the average ultimate shear force. Also, for specimens made of clay burnt brick with mortar thickness 19 mm (Specimens- C-3/4, and C1-3/4), the average cracking lateral load is 4.77% of the average cracking shear force and the average ultimate lateral load is 12.09% of the average ultimate shear force. In the specimens made of machine brick with mortar thickness 13 mm (Specimens- M-1/2), the cracking lateral load is 4.28% of cracking shear force and the ultimate lateral load is 7.81% of ultimate shear force. Also, for specimens made of machine-made brick with mortar thickness of 19 mm (Specimens- M-3/4), the cracking lateral load is 3.78% of cracking shear force and the ultimate lateral load is 8.62% of ultimate shear force.

For Specimens-C-1/2 and C1-1/2, the average cracking horizontal load is 62% of the average cracking prism strength and the average ultimate prism strength is 93.3% of the average ultimate horizontal load. For Specimens-C-3/4 and C1-3/4, the average cracking horizontal load is 88.5% of the average cracking prism strength and the average ultimate prism strength is 77.6% of the average ultimate horizontal load. For Specimens-M-1/2, the cracking prism strength is 85.6% of the average cracking horizontal load and the ultimate horizontal

load is 70.5% of the average ultimate prism strength. For Specimens-M-3/4, the cracking horizontal load is 85.8% of cracking prism strength and the ultimate horizontal load is 67.0% of ultimate prism strength. For Specimens-C-1/2 and C1-1/2, the average cracking horizontal load is 99% of the average cracking shear strength and the average ultimate shear strength is 50.8% of the average ultimate horizontal load. For Specimens-C-3/4 and C1-3/4, the average cracking shear strength is 61.3% of the average horizontal load and the average ultimate shear strength is 24.1% of the average ultimate horizontal load. For Specimens-M-1/2, the cracking shear strength is 66.8% of the average cracking horizontal load and the ultimate shear strength is 33.8% of the average ultimate horizontal load. For Specimens-M-3/4, the cracking shear strength is 73.0% of the cracking horizontal load and the ultimate shear strength is 32.0% of the ultimate horizontal load.

Increasing mortar thickness prism ultimate strength increases 18.0% for clay burnt brick and with increasing mortar thickness prism ultimate strength increases by 1.3% for machine-made brick. Increasing mortar thickness ultimate shear strength decreases by 9.6% for clay burnt brick with frog mark and with increasing mortar thickness ultimate shear strength decreases by 8.0% for machine-made bricks without frog mark. In clay burnt brick shear strength is 12.5% more than machine-made brick. Increasing mortar thickness ductility decreases 22.0% for clay burnt brick and 20.0% for machine-made bricks. The average stiffness degradation of clay burnt brick with mortar thicknesses 13 mm and 19 mm are 20.0% and 13.93% per cycle respectively. The average stiffness degradation of machine-made brick with mortar thicknesses 13 mm and 19 mm is 18.68% and 18.21% per cycle. Energy absorbed by machine-made brick walls with a mortar thickness of 19 mm is 58.1% of the energy absorbed by machine-made brick walls with a mortar thickness of 13 mm. For specimens (C-1/2 & C1-1/2) and specimens (C-3/4 & C1-3/4), the average theoretical shear forces are 35.0% and 25.0% of the average tested lateral load. Also, for the specimen (M-1/2 & M1-1/2) and specimen (M-3/4 & M1-3/4), the average theoretical shear forces are 43.0% and 45.0% of the average tested lateral load. In terms of load bearing, ductility, and stiffness clay burnt brick performed better than machine-made brick. No relation between prism strength, shear strength, and wall stiffness was obtained since the failure mode of the wall is a combination of sliding and rocking. Full scale specimens may be investigated to get more accurate result. More parameters may be considered to achieve more specified result. Bond wrench test may be performed to compare with shear test result. Based on all the results, it is concluded that clay burnt brick is better than machine made brick.

Funding

This research did not receive any specific grant from funding agencies in the public, commercial, or non-profit sectors.

Conflicts of interest

The authors declare that they have no known competing financial interests or personal relationships that could have appeared to influence the work reported in this paper.

Authors contribution statement

The authors confirm their contribution to the paper as follows – M. R. Islam: data collection, analysis, draft manuscript preparation; A. Hasnat: draft manuscript preparation and interpretation of results; R. Ahsan: conception and design of the study; A. T. Alam: draft manuscript preparation.

References

[1] Drysdale RG, Hamid AA, Baker LR. Masonry structures: behavior and design. (No Title) 1994.

[2] Messali F, Esposito R, Jafari S, Ravenshorst G, Eguren PK, Rots J. A multiscale experimental characterisation of Dutch unreinforced masonry buildings. 16th Eur. Conf. Earthq. Eng., 2018.

[3] Bruneau M. State-of-the-Art Report on Seismic Performance of Unreinforced Masonry Buildings. J Struct Eng 1994;120:230–51. https://doi.org/10.1061/(ASCE)0733-9445(1994)120:1(230).

[4] Rehman MU, Ahmad M, Rashid K. Influence of fluxing oxides from waste on the production and physico-mechanical properties of fired clay brick: A review. J Build Eng 2020;27:100965. https://doi.org/10.1016/j.jobe.2019.100965.

[5] Borah B, Kaushik HB, Singhal V. Development of a Novel V-D Strut Model for Seismic Analysis of Confined Masonry Buildings. J Struct Eng 2021;147. https://doi.org/10.1061/(ASCE)ST.1943-541X.0002941.

[6] Polese M, Verderame GM, Mariniello C, Iervolino I, Manfredi G. Vulnerability Analysis for Gravity Load Designed RC Buildings in Naples – Italy. J Earthq Eng 2008;12:234–45. https://doi.org/10.1080/13632460802014147.

[7] Page AW. Finite Element Model for Masonry. J Struct Div 1978;104:1267–85. https://doi.org/10.1061/JSDEAG.0004969.

[8] Pandey BH, Meguro K. Simulation of brick masonry wall behavior under in-plane lateral loading using applied element method. 13th World Conf. Earthq. Eng., 2004, p. 1–6.

[9] Hasnat A, Ahsan R, Yashin SM. Quasi-static in-plane behavior of full-scale unreinforced masonry walls retrofitted using ferro-cement overlay. Asian J Civ Eng 2022;23:649–64. https://doi.org/10.1007/s42107-022-00447-7.

[10] Vasconcelos G, Lourenço PB. In-Plane Experimental Behavior of Stone Masonry Walls under Cyclic Loading. J Struct Eng 2009;135:1269–77. https://doi.org/10.1061/(ASCE)ST.1943-541X.0000053.

[11] Alecci V, Fagone M, Rotunno T, De Stefano M. Shear strength of brick masonry walls assembled with different types of mortar. Constr Build Mater 2013;40:1038–45. https://doi.org/10.1016/j.conbuildmat.2012.11.107.

[12] Léopold M, Désiré TJ, Germain M. Strength characteristics of earth bricks and their application in construction. Int Res J Eng 2014;2:1–7.

[13] Dabaieh M, Heinonen J, El-Mahdy D, Hassan DM. A comparative study of life cycle carbon emissions and embodied energy between sun-dried bricks and fired clay bricks. J Clean Prod 2020;275:122998. https://doi.org/10.1016/j.jclepro.2020.122998.

[14] Ikechukwu AF, Shabangu C. Strength and durability performance of masonry bricks produced with crushed glass and melted PET plastics. Case Stud Constr Mater 2021;14:e00542. https://doi.org/10.1016/j.cscm.2021.e00542.

[15] Hasnat A, Das T, Ahsan R, Alam AT, Ahmed H. In-plane cyclic response of

unreinforced masonry walls retrofitted with ferrocement. Case Stud Constr Mater 2022;17:e01630. https://doi.org/10.1016/j.cscm.2022.e01630.

[16] Hasnat A, Das T, Ahsan R, Alam AT, Ahmed H. Efficacy of Ferrocement at retrofitting URM walls. ResearchGate 2022. https://doi.org/10.13140/RG.2.2.15679.79525.

[17] S. Mohammed M. Finite Element Analysis of Unreinforced Masonry Walls. Al-Rafidain Eng J 2010;18:55–68. https://doi.org/10.33899/rengj.2010.31528.

[18] Ashraf M, Khan AN, Naseer A, Ali Q, Alam B. Seismic Behavior of Unreinforced and Confined Brick Masonry Walls Before and After Ferrocement Overlay Retrofitting. Int J Archit Herit 2012;6:665–88. https://doi.org/10.1080/15583058.2011.599916.

[19] El-Diasity M, Okail H, Kamal O, Said M. Structural performance of confined masonry walls retrofitted using ferrocement and GFRP under in-plane cyclic loading. Eng Struct 2015;94:54–69. https://doi.org/10.1016/j.engstruct.2015.03.035.

[20] Hegemier GA, Krishnamoorthy G, Nunn RO, Moorthy T V. Prism tests for the compressive strength of concrete masonry. Proc. North Am. Mason. Conf., vol. 1, 1978, p. 181–7.

[21] Concrete Masonry Prism Testing. ACI J Proc 1979;76. https://doi.org/10.14359/6957.

[22] Concrete Masonry Under Combined Shear and Compression Along the Mortar Joints. ACI J Proc 1980;77. https://doi.org/10.14359/7008.

[23] Brown R, Whitlock A. Compressive Strength of Grouted Hollow Brick Prisms. Mason. Mater. Prop. Perform., ASTM International100 Barr Harbor Drive, PO Box C700, West Conshohocken, PA 19428-2959; 1982, p. 99–117. https://doi.org/10.1520/STP30118S.

[24] Lee R, Longworth J, Warwanik J. Concrete masonry prism response due to load parallel to bed joints. Proc., 3rd North Am. Mason. Conf. Arlington, TX Univ. Texas, 1984.

[25] Wong H, Drysdale R. Compression Characteristics of Concrete Block Masonry Prisms. Mason. Res. Appl. Probl., ASTM International100 Barr Harbor Drive, PO Box C700, West Conshohocken, PA 19428-2959; 1985, p. 167–77. https://doi.org/10.1520/STP34554S.

[26] Khalaf FM. Blockwork Masonry Compressed in Two Orthogonal Directions. J Struct Eng 1997;123:591–6. https://doi.org/10.1061/(ASCE)0733-9445(1997)123:5(591).

[27] Haach VG, Vasconcelos G, Lourenço PB. Experimental Analysis of Reinforced Concrete Block Masonry Walls Subjected to In-Plane Cyclic Loading. J Struct Eng 2010;136:452–62. https://doi.org/10.1061/(ASCE)ST.1943-541X.0000125.

[28] Soon S. In-plane behaviour and capacity of concrete masonry infills bounded by steel frames 2011.

[29] Maheri MR, Najafgholipour MA, Rajabi AR. The influence of mortar head joints on the in-plane and out-of-plane seismic strength of brick masonry walls 2011.

[30] Venkatarama Reddy B V., Uday Vyas C V. Influence of shear bond strength on compressive strength and stress–strain characteristics of masonry. Mater Struct 2008;41:1697–712. https://doi.org/10.1617/s11527-008-9358-x.

[31] Yi W-H, Oh S-H, Lee J-H. Shear capacity assessment of unreinforced masonry wall. 13th World Conf. Earthq. Eng., 2004, p. 1–12.

[32] Churilov S, Dumova-Jovanoska E. In-plane shear behaviour of unreinforced and strengthened masonry walls, Macedonian Association of Earthquake Engineering; 2010.

[33] Ali Q, Badrashi YI, Ahmad N, Alam B, Rehman S, Banori FAS. Experimental

investigation on the characterization of solid clay brick masonry for lateral shear strength evaluation. Int J Earth Sci Eng 2012;5:782–91.

[34] Voon KC, Ingham JM. Experimental In-Plane Shear Strength Investigation of Reinforced Concrete Masonry Walls. J Struct Eng 2006;132:400–8. https://doi.org/10.1061/(ASCE)0733-9445(2006)132:3(400).

[35] Maheri MR, Sherafati MA. The effects of humidity and other environmental parameters on the shear strength of brick walls: evaluation of field test data. Mater Struct 2012;45:941–56. https://doi.org/10.1617/s11527-011-9809-7.

[36] BSTI. BDS EN197-1:2003 2005.

[37] Priestley MJN, Seible F, Calvi GM. Seismic Design and Retrofit of Bridges. Wiley; 1996.

[38] Hose Y, Silva P, Seible F. Development of a Performance Evaluation Database for Concrete Bridge Components and Systems under Simulated Seismic Loads. Earthq Spectra 2000;16:413–42. https://doi.org/10.1193/1.1586119.